



## Enhanced Photovoltaic System by Implementing Fuzzy Logic MPPT Strategy for Control of Four-Switch Z-Source Inverter

Ouledali Omar<sup>1</sup>, Bouzidi Mohammed<sup>2</sup>, Nasri Abdelfatah<sup>3</sup>, Achar Abdelkader<sup>1</sup>, Abdelaoui Moustapha<sup>1</sup>, Hamouda Messaoud<sup>1</sup>

<sup>1</sup>Sustainable Development and Informatics Laboratory (LDDI), Faculty of Science and Technology, University of Adrar, 01000, Algeria.

EMAIL:ouleomar@yahoo.fr;achar.kada@gmail.com;mabdelaoui@yahoo.com;jhamouda@yahoo.fr

<sup>2</sup>Department of Sciences and Technology, Faculty of Sciences and Technology, University of Tamanrasset, Sersouf P.O. Box 10034, Tamanghasset 11001, Algeria

EMAIL:m.bouzidi@univ-tam.dz

<sup>3</sup>Laboratory Smart Grid and Renewable Energy SGRE, University Tahri Mohamed Bechar, BP 417 road kenadza Béchar 08000 Algeria.

EMAIL:nasri.abdelfatah@univ-bechar.dz

**Abstract:** -This study aims to enhance the efficiency of a conventional inverter by analyzing a Z-source, four-switch, three-phase system connected to a PV generator. This system allows the transmission of electricity to the power grid. In addition, this inverter is more efficient due to its integration of the booster chopper and inverter functions into a single stage. We also employed a space-vector pulse-width modulation (S.V.P.W.M.) control approach to regulate the F.S.T.P. and Z-source inverters. We enhance the Z-source network by adding a shoot-through state, which reduces Total Harmonic Distortion (THD) and improves efficiency. The solar generator (G.P.V.) achieves its maximum power output through fuzzy logic and the highest Power Point Tracking (MPPT) approach. We generated simulator results using the M.A.T.L.A.B. Simulink software to assess the validity of the proposed research.

**Keywords:** Z-source four switches three-phase inverter, photovoltaic generator (G.P.V.), shoot-through State, PWM Control, MPPT technique, fuzzy logic.

### 1. Introduction

Integrating solar energy into the power grid presents technological challenges due to the intermittent nature of renewable energy sources. The characteristics of solar energy are diverse. The inclusion of solar energy into the electricity system presents technological challenges due to its sporadic and unpredictable characteristics, complicating its integration into the electrical grid [1, 2]. Because it is subject to variations, implementing appropriate



adaptation strategies is required to ensure that this resource is effectively used for various applications and that high-quality energy transfer is achieved. In modern electrical energy conversion devices, static converters and control systems are necessary to overcome these issues. [3, 4, 5, 6]. Converting the variable output of solar panels into electricity that is adequate for power converters. To guarantee a high level of conversion efficiency, trustworthiness, and consistency in the energy supply, control systems play an extremely important role[7,8,9]. The Z-source inverter has effectively resolved the challenges of conventional voltage source inverters (V.S.I.) in power conversion applications, including DC-AC, AC-DC, and DC-DC. [10,11]. The primary circuit of the linked to the power supply via a unique impedance network, which provides characteristics absent in conventional Voltage Source Inverters (VSI)[12,13,15].Implementing a four-switch three-phase inverter (F.S.T.P.I.) significantly decreases the presence of harmonics, electromagnetic interference, and common-mode noise. As a result, it is well-suited for adjustable induction motor drive systems and surpasses traditional Voltage Source Inverters (V.S.I.) in This unique approach has also enhanced DC-to-AC voltage amplification and conversion in fuel cell devices. The present research focuses on analyzing the performance and efficiency of a new topology that combines a Z-source inverter with F.S.T.P.I.

## 2. Modeling of PV panels and MPPT Control

### 2.1. Modeling of PV Panels

Photovoltaic (PV) cells consist of numerous P-N junctions capable of converting light into electrical energy. The fundamental properties of PV cells resemble those of diodes. The basic circuit of a typical PV model has a photocurrent, a diode, a parallel resistor for leakage current, and a series resistor that shows how much the current flow is resisted inside. [1,7] Figure 1.

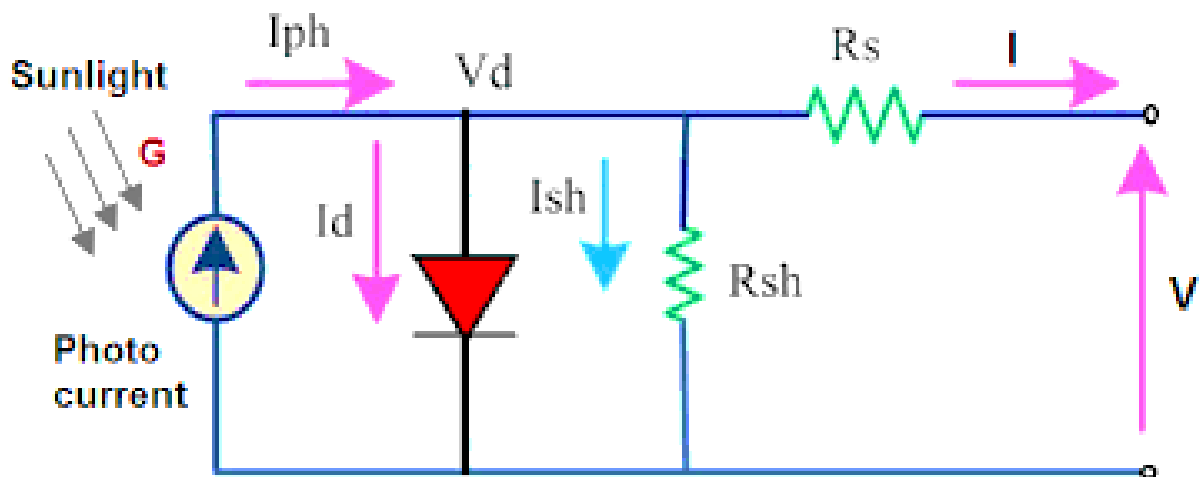


Figure1: PV module equivalent circuit



The voltage generated by a photovoltaic (PV) cell is directly influenced by the size of the current generated by light. This current, in turn, is influenced by the temperature and the intensity of the solar radiation. There is potential of showing the relationship [9, 19, 20]:

$$V = \frac{AkT}{e} \ln \frac{I_{ph} + I_0 - I}{I_0} - R_s I \quad (1)$$

Where:

$I_{ph}$ : Photo Current is defined by:

$$I_{ph} = [I_{sc} + K_1(T_c + T_{ref})] * H \quad (2)$$

$I_{rs}$ : Reverse Saturation Current is presented as:

$$I_{rs} = \frac{I_{cs}}{\exp \frac{qV_{oc}}{N_s k A T} - 1} \quad (3)$$

$I_0$ : Diode Saturation Current is established:

$$I_0 = I_{rs} * \left(\frac{T}{T_r}\right)^3 * \exp \left[ \left( \frac{q * E_{go}}{A * k} \right) * \left( \frac{1}{T_r} - \frac{1}{T} \right) \right]; \quad (4)$$

$I$ : Output current is given by:

$$I_{pv} = N_p I_{ph} - N_p I_0 \left[ \exp \left( \frac{q * (V_{pv} + I_{pv} R_s)}{N_s * A * k * T} \right) - 1 \right] \quad (5)$$

## 2.2. MPPT Control Technique

### 2.2.1 The Principle of MPPT Techniques

Maximum Power Point Tracking (MPPT) control facilitates the continuous extraction of optimal power from a photovoltaic (PV) generator, per its definition. Irrespective of varying weather conditions, such as temperature and irradiation, as well as battery voltage or load fluctuations, the converter control ensures that the system consistently operates at its maximum efficiency point [21, 22]. Figure 2.

A DC/DC converter is utilised within the control section of the photovoltaic system due to its ease of manipulation via duty cycles using a PWM signal. In our study, a boost chopper is the power interface, which the MPPT controller regulates. The objective is to adjust the chopper's output voltage to align with the voltage requirements of the load. [22,23].

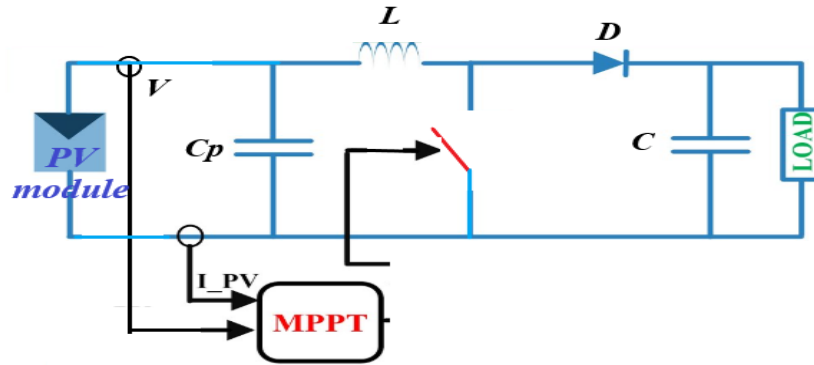


**Figure2: Circuit diagram of a Boost converter**

*A) Perturb and Observe (P&O) method*

This approach introduced a perturbation to the current voltage applied to the module. This voltage fluctuation alters the power output. Additional disturbance towards lower voltages is necessary to reach the maximum power point (M.P.P.). Therefore, the algorithm will gradually approach the Maximum Power Point (M.P.P.) through multiple perturbations. The diagram below encapsulates the essence of this notion [1, 2, 5].

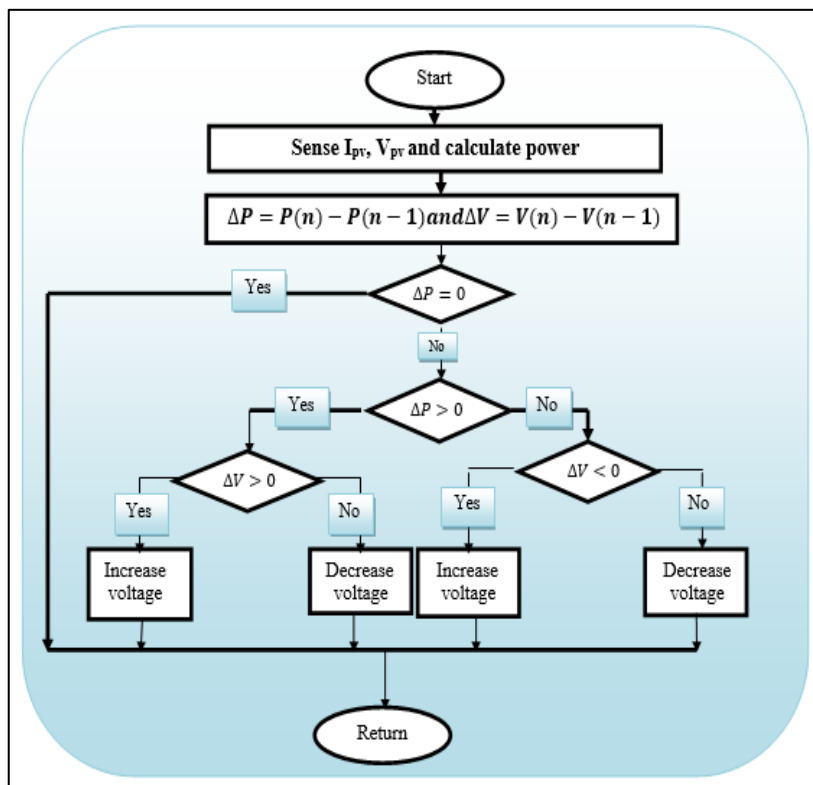


**Figure 3: P&O algorithm**



## 2.2.2 Implementation of Fuzzy Logic MPPT Algorithm

To use the MPPT strategy based on fuzzy logic, it is not necessary to know the system model. For the fuzzy logic controller, the system error (E) and the change in error (C.E.) are the inputs considered. The equations that follow define E and C.E. [17,20,21]:

$$E(k) = \frac{\Delta I}{\Delta V} + \frac{I}{V} = \frac{\Delta P}{\Delta V} = \frac{\Delta P}{\Delta I} \quad (6)$$

$$CE(k) = E(k) - E(k - 1) \quad (7)$$

$$\text{With: } \Delta I = I(k) - I(k - 1) \quad (8)$$

$$\Delta V = V(k) - V(k - 1) \quad (9)$$

The fuzzy logic structure :

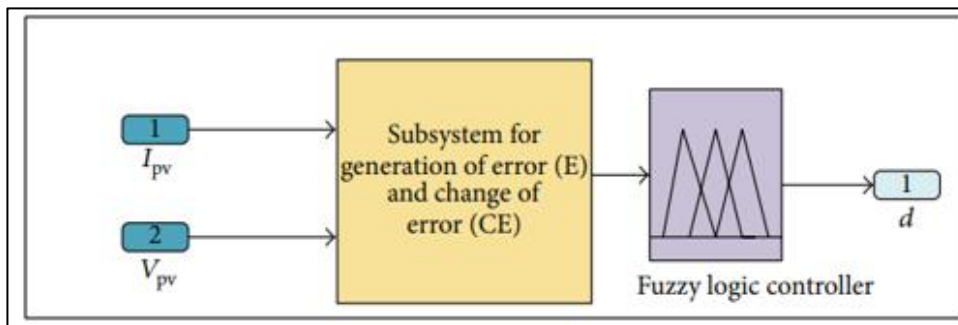
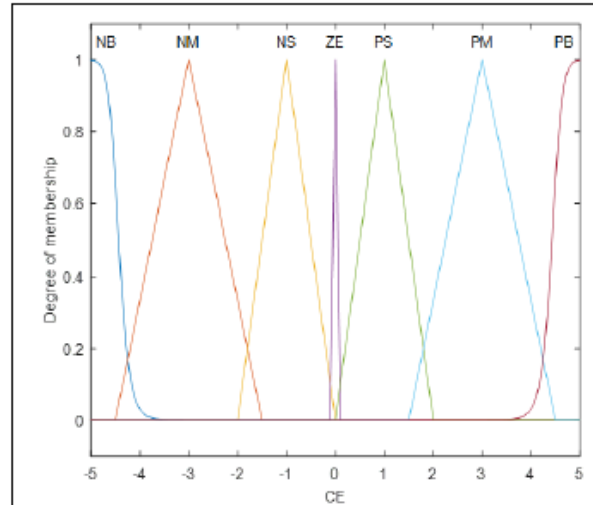
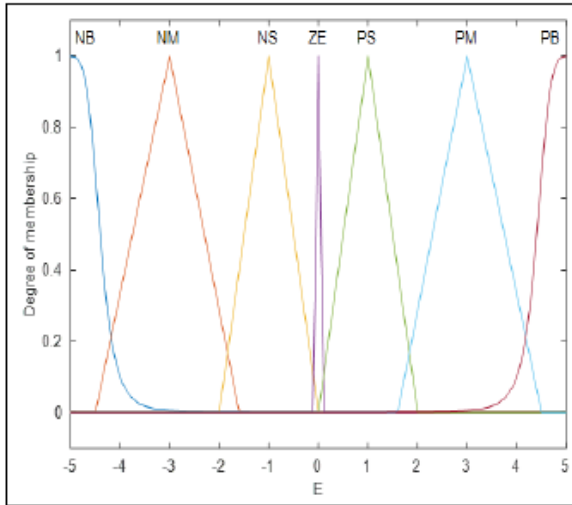


**Figure4: External block view of the fuzzy logic algorithm.**

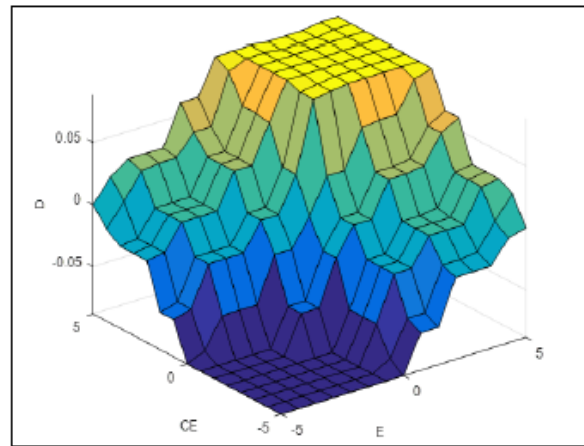
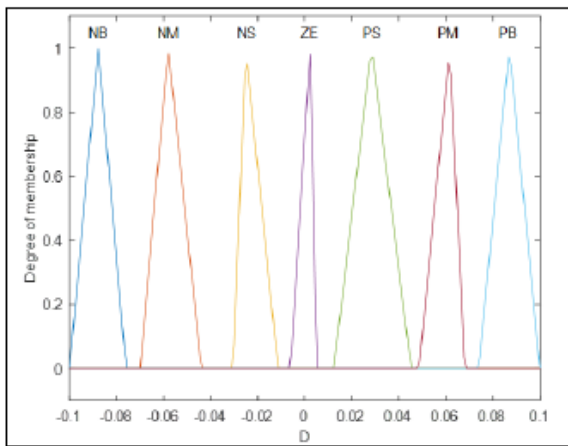
## 2.2.3 The setting of fuzzy rules

**Table 1: Fuzzy rules base**

C.E.	NB	NM	NS	ZE	PS	PM	PN
E	NB	NM	NS	ZE	PS	PM	PN
NB	NB	NB	NB	NB	NM	NS	ZE
NM	NB	NM	NM	NM	NS	ZE	PS
NS	NB	NM	NS	NS	ZE	PS	PM
ZE	NB	NM	NS	ZE	PS	PM	PB
PS	NM	NS	ZE	PS	PM	PM	PB
PM	NS	ZE	PS	PM	PM	PB	P.B.
PN	ZE	PS	PM	PB	P.B.	P.B.	P.B.



(a) Membership function for the error " E " signal (b) Membership function for error " CE "



(c) Membership function for duty cycl

(d) Surface fuzzy input of output functions

**Figure5: Membership functions inputs, outputs, and Surface of fuzzy of output functions**

### 3. Analysis of Z-source network

The Z-source inverter is used to address the issues found in traditional inverters and utilises a unique impedance network that connects the inverter's main circuit to the power source. This inverter has unique features compared to conventional sources [24, 25].

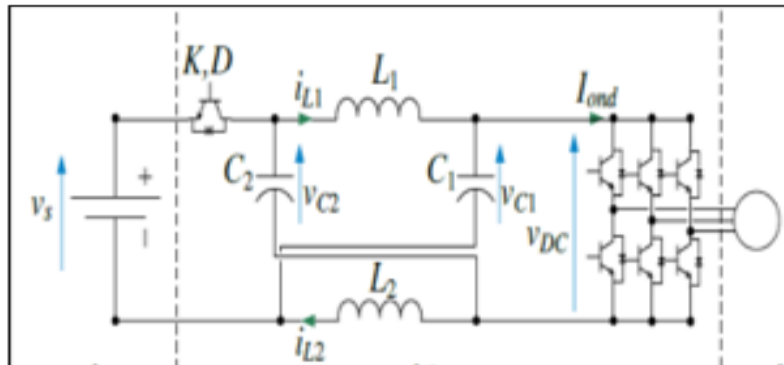


**Figure6: The equivalent circuit of the Z-source inverter viewed from the DC link**

We assume that the inductors ( $L_1$  and  $L_2$ ) and capacitors ( $C_1$  and  $C_2$ ) have the same inductance and capacitance values, respectively, from Figure .6.

$$\begin{cases} V_{L1} = V_{L2} = V_L \\ \text{and} \\ V_{C1} = V_{C2} = V_C \end{cases} \quad (10)$$

The Z-source network uses two modes of operation to achieve boost and inversion in a single stage.

*a-Shoot-through state (S.T.S.)*

The Z.S.I. advantageously uses the shoot-through states to boost the DC bus voltage by gating on a phase leg's upper and lower switches. [ 10,12,26]

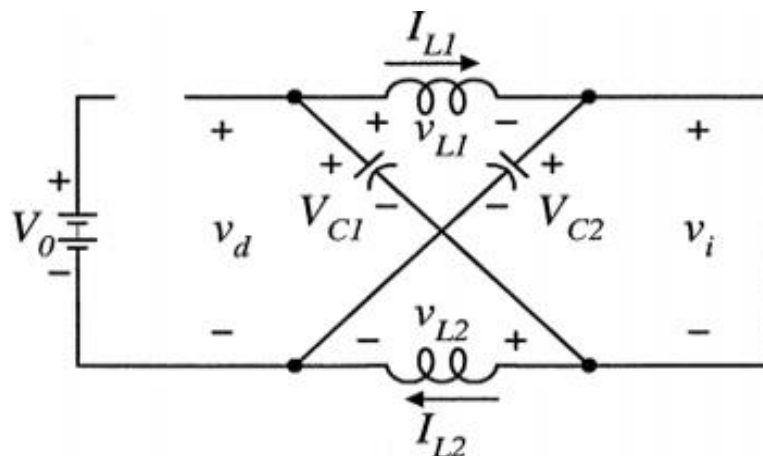


**Figure 7:Equivalent circuit shoot-through zero state of the Z.S.I.**

As a result, the capacitor voltage is boosted during this state, the sum of the two capacitor voltages is greater than the DC source voltage ( $V_{C1}+V_{C2} > V_0$ ), the diode is reverse-biased, and the capacitors charge the inductors. The voltages across the inductors are



$$\begin{cases} V_{L1} = V_{C1} \\ \text{and} \\ V_{L2} = V_{C2} \end{cases} \quad (11)$$

The inductor current increased linearly, assuming the capacitor voltage was constant during this period. Because of the symmetry ( $L_1=L_2=L$ ) and ( $C_1=C_2=C$ ) of the circuit, ( $V_{L1}=V_{L2}=V_L$ ), ( $I_{L1}=I_{L2}=I_L$ ) and ( $V_{C1}=V_{C2}=V_C$ ) [3,6]

This means,

$$V_C = V_L, V_D = 2V_C \text{ and } V_i = 0 \quad (12)$$

*b- Active state (Non-shoot-Through State)*

The inverter is in a non-shoot-through state, and the inductor current satisfies the following equation [1,3]:

$$I_L > \frac{1}{2}I_i \quad (13)$$

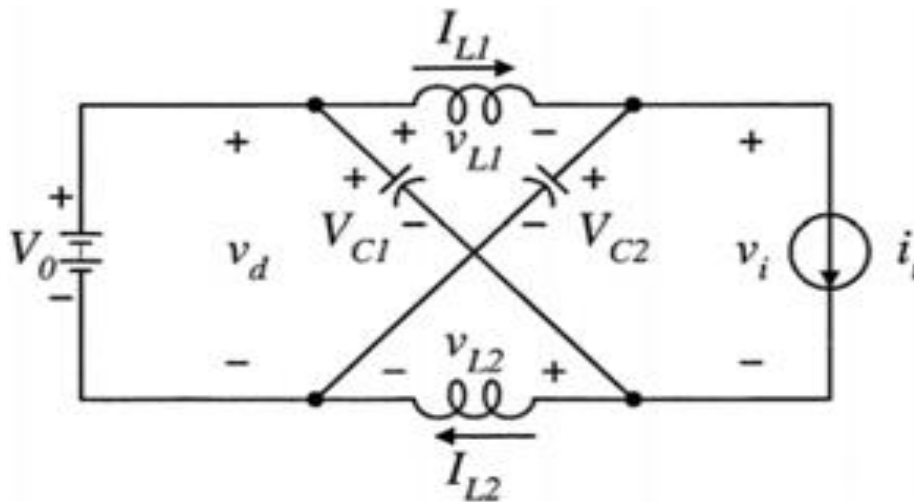


**Figure8: The Z.S.I.'s equivalent circuit non-shoot-through zero state**

Because of the symmetry of the circuit, the capacitor currents  $I_{C1}$  and  $I_{C2}$  and the inductor currents  $I_{L1}$  and  $I_{L2}$  should be equal. In this Mode, the input current from the DC source becomes:[13,14]

$$I_{in} = I_{L1} + I_{C1} = I_{L1} + I_{L2} - I_i = I_L - I_i > 0 \quad (14)$$

Therefore, the diode is conducting, and the voltage across the inductor is.

$$V_L = V_0 - V_c \quad (15)$$



### 3.1. Four Switch Three Phase Inverter (F.S.T.P.I.)

The main power circuit of the F.S.T.P.I. fed resistive load is shown in Figure 9; four switches,  $q_1$ ,  $q_2$ ,  $q_3$ , and  $q_4$ , and DC link capacitors  $C_1$  and  $C_2$  are employed in this circuit. Phases « a » and « b » are taken from the legs with the switches. Phase « c » is connected to the midpoint of the two DC-link capacitors [27,9]

The assumed stiff voltage available across the two DC-link capacitors is:

$$V_{c1} = V_{c2} = \frac{V_{dc}}{2} \quad (16)$$

Where  $V_{dc}$  corresponds to a stiff DC-link voltage, and  $V_1$ ,  $V_2$ , and  $V_3$  pole voltages depend on the switching states of the power switches in the inverter, which can be expressed in terms of the binary variables  $q_1$  and  $q_2$  and the DC-link voltage as follows:

$$V_1 = 2q_1 - \frac{V_{dc}}{2} \quad (17)$$

$$V_2 = 2q_2 - \frac{V_{dc}}{2} \quad (18)$$

$$V_3 = 0 \quad (19)$$

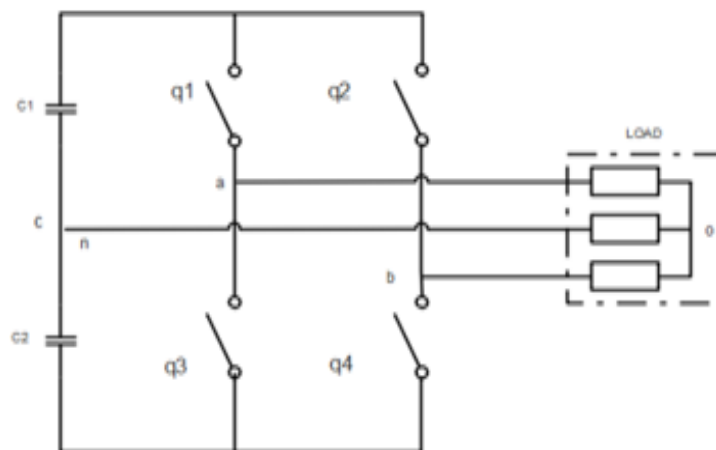


Figure9: Three-Phase Four-Switch Inverter

Table 2 Switching Functions and the Output Voltages of

Switching Function		Switch on	Output Voltage Vector		
$q_1$	$q_2$	$T_1 = q_1,$ $T_3 = q_2$ $T_4 = T_2$	$V_1$	$V_2$	$V_3$

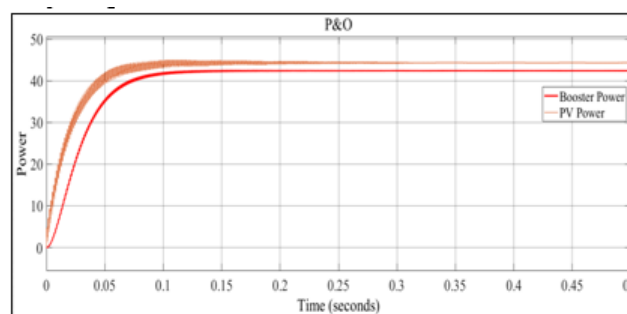


0	0	$T_2$	$T_4$	$\frac{-V_{dc}}{3}$	$\frac{-V_{dc}}{3}$	$\frac{2V_{dc}}{3}$
0	1	$T_2$	$T_3$	$-V_{dc}$	$V_{dc}$	0
1	0	$T_1$	$T_4$	$V_{dc}$	$-V_{dc}$	0
1	1	$T_1$	$T_3$	$\frac{V_{dc}}{3}$	$\frac{V_{dc}}{3}$	$\frac{-2V_{dc}}{3}$

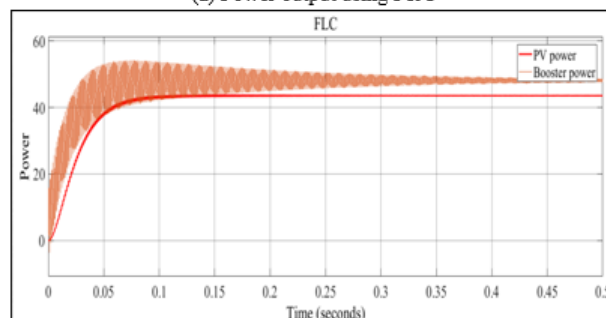
The entries in the table are related to the output voltage vector corresponding to each switching function

#### 4.Results

Despite rapid temperature fluctuations, the P&O algorithm effectively controlled the Maximum Power Point (M.P.P.). The controller efficiently monitored and upheld the new M.P.P. Figure 10. The observed minor reduction in power from the solar panel to the boost converter output is mostly attributable to switching losses and losses in the inductor and capacitor of the boost converter. We noted anomalies in the fuzzy-logic controller's photovoltaic voltage and power output. The swift reaction of the FLC produced these problems. Nonetheless, these disturbances do not influence the setting time, which is shorter than the P&O duration.



(a) Power output using P&O



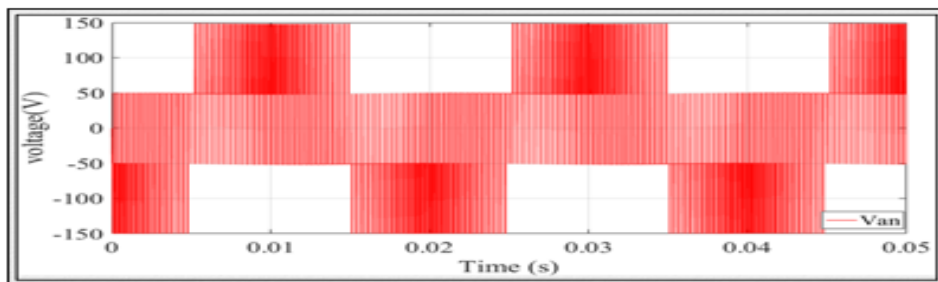
(b) Power output using FLC

Figure 10: MPPT Results.

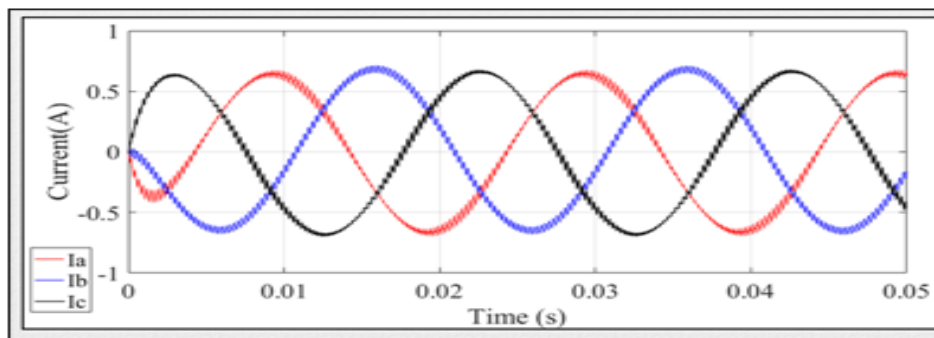


The voltage waveform from the line to neutral, shown in Figure 11 (a), shows  $V_{an}$  with an R.L. load ( $R=10 \Omega$ ,  $L=1 \text{ mH}$ ) and a modulation index (MI) of 0.8. The wave has a complicated shape because of the strong, higher-order harmonics (5th, 7th, and 11th). The sinusoidal shape is complex owing to the high-amplitude, higher-order harmonics (5th, 7th, and 11th).

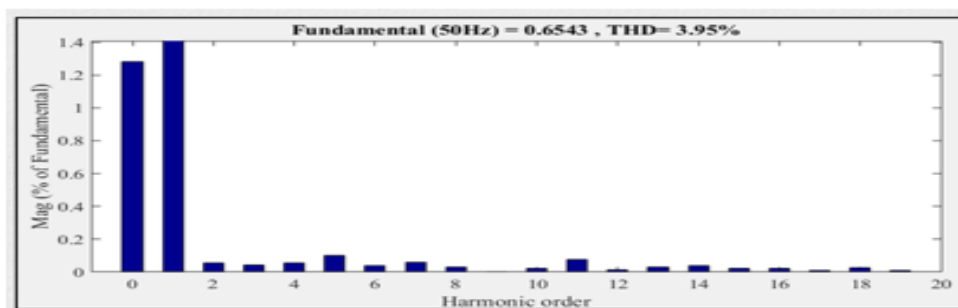
Figure 11 (b) illustrates the waveform of the three-phase current output produced by the F.S.T.P. Z source inverter. The output generally exhibits a sinusoidal shape, which is attributed to the accurate control technique and the limited number of switches. However, minor disturbances were present owing to the presence of higher-order harmonics.



(a) Voltage output of phase  $V_a$  of F.S.T.P.Z.I.



(b) Three-phase current output of F.S.T.P.Z.I.



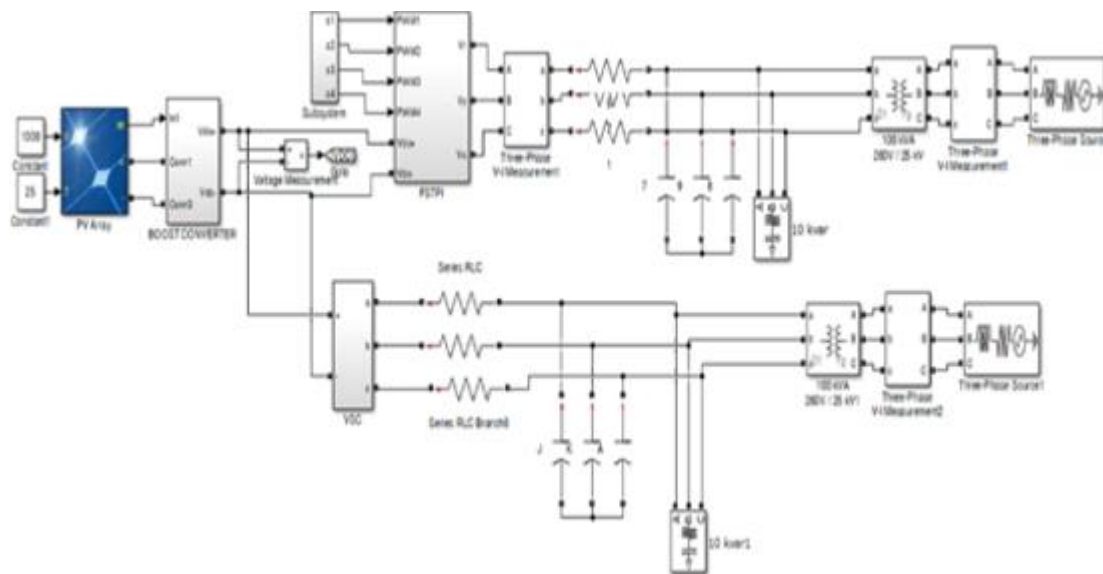
(c) FFT Analysis

Figure 11: F.S.T.P.Z.I. outputs and FFT Analysis



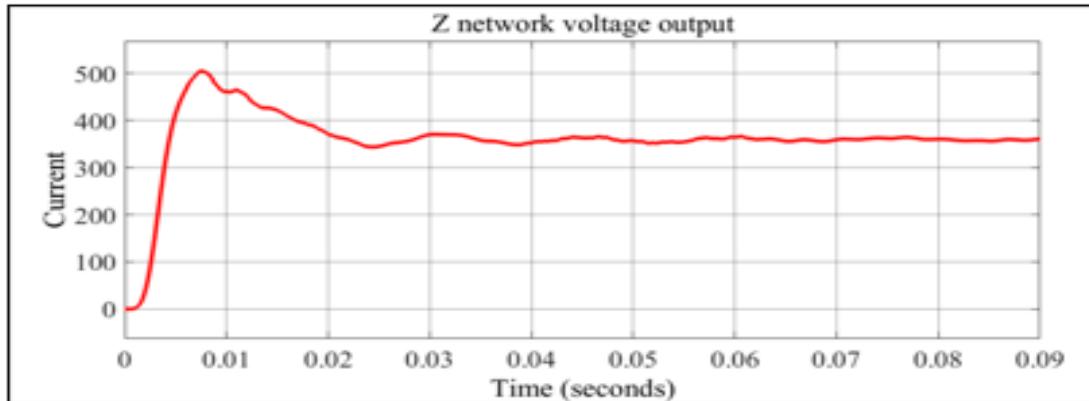
In Figure 11(c), high-order harmonics are present and can be eliminated by incorporating a primary low-pass filter. This enhances the Total Harmonic Distortion (THD). The design of this filter will be discussed in the upcoming chapter, which will connect the F.S.T.P. Z-source inverter to the power grid.

Figure 12 shows the process of generating electricity from a PV system and delivering it to a 3-phase power grid. The system contains a 100 kW PV Array, Boost converter with MPPT (P&O) connected to an F.S.T.P. Z-source inverter and VSC, an RC Filter, transformer 100 KVA 250 V/25 KW, and a three-phase power grid.

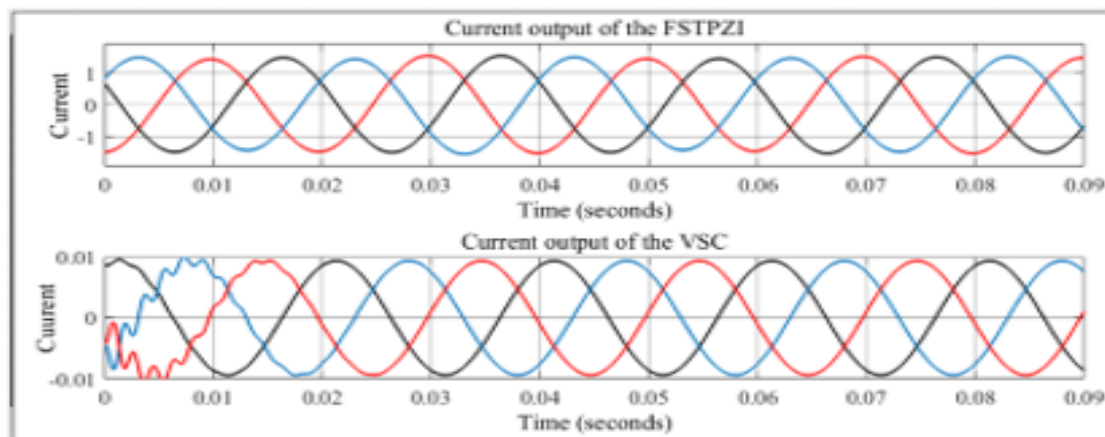


**Figure 12: Model F.S.T.P. Z-source inverter and VSC connected with power grid**

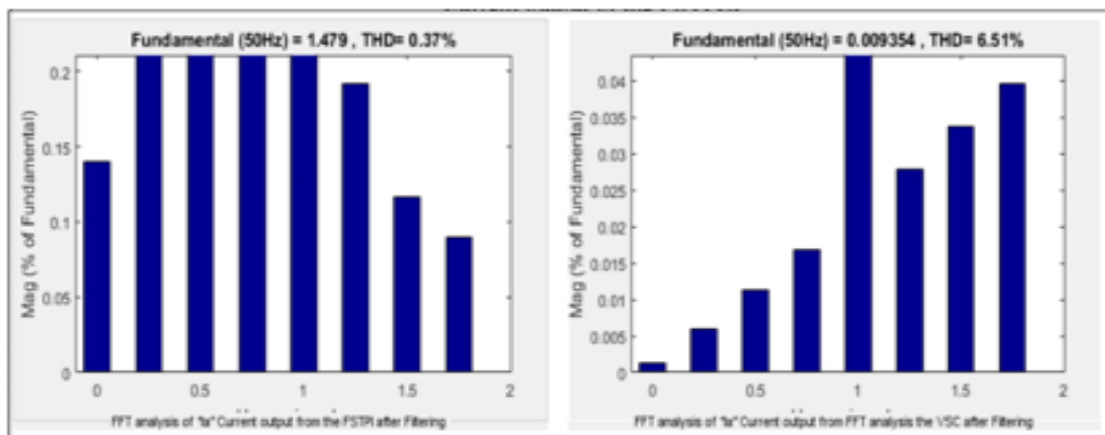
The simulation results show that the FSTP ZSI can produce a smooth sinusoidal load current without needing a filter, with a total harmonic distortion (THD) of 4%. This is a significant achievement considering the absence of a filter. In addition, the results confirm that the output voltage aligns with the design analysis. We successfully linked the PV and F.S.T.P. Z-source inverter to a power grid and compared its performance with the traditional VSC. These findings indicate that the F.S.T.P., when equipped with a basic R.C. filter, the Z-source inverter outperformed the VSC with respect to distortion (THD). Specifically, the F.S.T.P. Z-source inverter achieved a THD of 0.3%, whereas the VSC recorded a THD of 6%, which is even worse than the results obtained from the F.S.T.P. Z-source inverter without a filter. The F.S.T.P. Z-source design showed it was better in terms of being affordable, smaller in size, easier to control, having less power loss, being able to handle changes from the MPPT controller, and its ability to increase voltage.



(a) The output voltage of the Z network



(b) Current output of the F.S.T.P.Z.I. after Filtering



(c) FFT analysis of Current "Ia"

Figure13: The output from the F.S.T.P.I. and the VSC after Filtering



## 5.CONCLUSION

This paper introduced a new three-phase inverter topology, the F.S.T.P.I., which reduces harmonic distortion very well, as well as the operating principle of the z-source inverter and optimal management technique. The input voltage can be increased without a step-up converter with a z-source inverter. Moreover, we established a connection between a photovoltaic (PV) system and a floating-switch three-phase (F.S.T.P.) The Z-source inverter uses a Space Vector Modulation (SVM) technique and is integrated with a power grid. The results demonstrate the seamless integration of these blocks, as evidenced by the sinusoidal waveform of the voltage and current entering the Grid from the F.S.T.P.I. Furthermore, the power quality is nearly ideal compared with the conventional VSC, indicating that achieving a superior output would require the implementation of a significantly costlier filter.

## References

- [1] Sadki, W., Ferouhat, W., ‘Control of the Four Switch Z-source Three Phase Inverter Integrated in a Photovoltaic system’, Master dissertation, University Ahmed DRAIA of Adrar, 2021.
- [2] Kalaiarasi, N., Sivapriya, A., Vishnuram, Pradeep, et al., ‘Performance Evaluation of Various Z-Source Inverter Topologies for PV Applications Using AI-Based MPPT Techniques’, International Transactions on Electrical Energy Systems, 2023, vol. 2023, no 1, p. 1134633.
- [3] Chen, D., Zhao, J., et QIN, S. ‘SVM strategy and analysis of a three-phase quasi-Z-source inverter with high voltage transmission ratio’, Science China Technological Sciences, 2023, vol. 66, no 10, p. 2996-3010.
- [4] Zaghba, L., et al., ‘Enhancing grid-connected photovoltaic system performance with novel hybrid MPPT technique in variable atmospheric conditions’, Scientific Reports, 2024. 14(1): p. 8205.
- [5] Bettahar, F., et al., ‘A comparative study of PSO, GWO, and HOA Algorithms for Maximum Power Point Tracking in partially shaded Photovoltaic systems’, Power Electronics and Drives, 2024. 9.
- [6] Bettahar, F., S. Abdeddaim, and B. Achour, ‘Enhancing PV Systems with Intelligent MPPT and Improved control strategy of Z-Source Inverter’, Power Electronics and Drives, 2024. 9.
- [7] Husam Ali Hadi, Abdallah Kassem, Hassan Amoud, Safwan Nadweh, ‘Improve power quality and stability of Grid - Connected PV system by using series filter’, Heliyon, Volume 10, Issue 21,2024,



- [8] Vendoti, S., et al., 'Grid connected improved sepic converter with intelligent strategy for energy storage system in railway applications', *Scientific Reports*, 2025. 15(1): p. 13192.
- [9] Boubii, C., et al., 'Synergizing wind and solar power: An advanced control system for grid stability', *Sustainability*, 2024. 16(2): p. 815.
- [10] Kalaiarasi, N., et al., 'Performance Evaluation of Various Z-Source Inverter Topologies for PV Applications Using AI-Based MPPT Techniques', *International Transactions on Electrical Energy Systems*, 2023. 2023(1): p. 1134633.
- [11] Samanbakhsh, R., et al., 'A Z-source inverter with switched network in the grid-connected applications', *International Journal of Electrical Power & Energy Systems*, 2023. 147: p. 108819.
- [12] Maheswari, K., R. Bharani Kumar, and S. Manivannan, 'Comparative evaluation of Z source/quasi-Z-source direct and indirect matrix converters for PMG based WECS', *Results in Engineering*, 2024. 22: p. 102219
- [13] Monjo, L., et al., 'Quasi-Z-source inverter-based photovoltaic power system modeling for grid stability studies', *Energies*, 2021. 14(2): p. 508.
- [14] Zarei, G., et al., 'High voltage gains switched z-source inverter with low current stress', *IET Power Electronics*, 2024. 17(1): p. 38-53
- [15] K. Jäger, O. Isabella, A.H.M. Smets, R. A.C.M.M. Van, Swaij and M. Zeman, 'Solar energy fundamentals, technology, and systems', copyright delft university of technology, 2014
- [16] Ilyas, A., Khan, M. R., & Ayyub, M., 'FPGA based real-time implementation of fuzzy logic controller for maximum power point tracking of solar photovoltaic system', *Optik*, 2020, vol. 213, p. 164668.
- [17] Ali, M. N., Mahmoud, K., Lehtonen, M., & Darwish method, M. M. An efficient fuzzy-logic based variable-step incremental conductance MPPT for grid-connected PV systems. *Ieee Access*, 2021, vol. 9, p. 26420-26430.
- [18] Fathi, M., & Parian, J. A., 'Intelligent MPPT for photovoltaic panels using a novel fuzzy logic and artificial neural networks based on evolutionary algorithms', *Energy Reports*, 2021, vol. 7, p. 1338-1348.
- [19] Chen, M., Loh, P. C., Yang, Y., & Blaabjerg, F., 'A six-switch seven-level triple-boost inverter', *IEEE Transactions on Power Electronics*, 2020, vol. 36, no 2, p. 1225-1230.



- [20]Morey, M., Gupta, N., Garg, M.M. et al., ‘Experimental investigation of ANFIS-PSO MPPT control with enriched voltage gain DC–DC converter for grid-tied PV applications’*Electr Eng* (2024). <https://doi.org/10.1007/s00202-023-02192-9>
- [21] Youcef, H., Touhimi, G., Omar, O., Essama, G. a., & Slimane, L, ‘Sliding Mode based PSO MPPT for Solar PV System’, *PrzegladElektrotechniczny*, 2024, vol. 2024, no 1.
- [22]G. Touhami, ‘Optimization of a hybrid system (PV-fuel cell) of energy production for an isolated site’, *SEES*, vol. 5, no. 1, pp. 2319–2332, May 2024.
- [23]Jamaaoui, F., Puig, V., & Ayadi, M. ‘Optimal Control of Hybrid Photovoltaic/Thermal Water System in Solar Panels Using the Linear Parameter Varying Approach’, *Processes*, 2023, vol. 11, no 12, p. 3426.
- [24]Scarabelot, L.T., G.A. Rampinelli, and C.R. Rambo, ‘Overirradiance effect on the electrical performance of photovoltaic systems of different inverter sizing factors’, *Solar Energy*, 2021. 225: p. 561-568.
- [25]Shaik, F., S.S. Lingala, and P. Veeraboina, ‘Effect of various parameters on the performance of solar PV power plant: a review and the experimental study’, *Sustainable Energy Research*, 2023. 10(1): p. 6.
- [26]Wang, Y. and L. Sun, ‘Photovoltaic Maximum Power Point Tracking Technology Based on Improved Perturbation Observation Method and Backstepping Algorithm’, *Electronics*, 2024. 13(19): p. 3960.
- [27] Bettahar, F., S. Abdeddaim, and B. Achour, ‘Enhancing PV Systems with Intelligent MPPT and Improved control strategy of Z-Source Inverter’, *Power Electronics and Drives*, 2024. 9.